



Iranian Research Organization  
for Science and Technology  
(IROST)

Advances  
Environmental  
Technology



Journal home page: <https://aet.irost.ir/>

# ZnS and ZnS/ZnO assembly for photocatalytic removal of Reactive Red 66

Shabnam Sheshmani\*, Mahan Mardali, Ashraf S. Shahvelayati, Leila Hajiaghababaei

Department of Chemistry, College of Basic Sciences, Yadegar-e-Imam Khomeini (RAH) Shahre Rey Branch, Islamic Azad University, Tehran, Iran

## ARTICLE INFO

### Document Type:

Research Paper

### Article history:

Received 29 May 2023

Received in revised form

19 August 2023

Accepted 21 August 2023

### Keywords:

ZnS

ZnS/ZnO heterostructure

Reactive Red 66

Photocatalytic degradation

## ABSTRACT

The current work investigated the effect of ZnS and ZnS/ZnO assembly on the photocatalytic removal of Reactive Red 66 from an aqueous solution. The photocatalytic activities were carried out using both UV irradiation and visible light, and the effects of various operating parameters, such as pH, catalyst loading, dye concentration, and contact time, were studied. The results showed that the ZnS/ZnO heterostructure exhibited a higher dye removal percentage than ZnS alone and assisted in the photodegradation of Reactive Red 66. Maximum adsorption was found at pH 2 and 5, indicating that the dye removal was strongly pH-dependent. The highest dye removal efficiency under UV light was 77.7 and 91.7% using ZnS and ZnS/ZnO, respectively. Furthermore, the degradation percentage of Reactive Red 66 by ZnS and ZnS/ZnO decreased to 43.3 and 75.2% under visible light. The enhanced photocatalytic activity of the ZnS/ZnO heterostructure is attributed to its high absorption of light, efficient separation of electron-hole pairs, and quick surface reaction in the heterostructure.

## 1. Introduction

Industrialization has brought immense economic prosperity but has also led to severe environmental degradation, including water and air pollution, loss of natural resources, and climate change. This can be attributed to the unregulated release of hazardous contaminants, such as dyes, chemicals, heavy metals, organic solvents, petroleum products, and solid wastes, into the environment. The widespread problem of environmental pollution significantly impacts human health, living organisms, and ecosystems. To address this issue,

it is necessary to completely convert the harmful compounds to eliminate their toxicity and persistence. Photocatalytic processes have gained attention as a potential solution for environmental remediation [1,2]. Photocatalytic degradation is an advanced process that utilizes light absorption to generate electron-hole pairs, which then initiate the degradation process [3]. First, the hole in the valence band oxidizes absorbed water molecules or hydroxide ions to create hydroxyl radicals. Then, the electron in the conductive band reduces oxygen molecules to produce hydroperoxyl or superoxide

\*Corresponding author Tel.: +982155229209

E-mail: shabnam\_sheshmani@yahoo.com

DOI:10.22104/AET.2023.6309.1734

COPYRIGHTS: ©2023 Advances in Environmental Technology (AET). This article is an open access article distributed under the terms and conditions of the Creative Commons Attribution 4.0 International (CC BY 4.0) (<https://creativecommons.org/licenses/by/4.0/>)

radicals [4,5]. During photocatalytic degradation, these reactive species react with adsorbed pollutant molecules and convert them to harmless products [6-8]. In addition to pollutant degradation, photocatalysts have also been used for other applications, such as antifouling [9], anti-fogging [10], self-cleaning [11], air purification [12], and wastewater treatment [13]. The photodegradation efficiency of photocatalysts has been improved in recent years through metal loading, metal doping, metal implantation, and heterostructure design [14]. However, the particle shape, particle size, surface area, crystal structure, and degree of crystallinity can also affect the photocatalytic efficiency [15,16]. Hybridizing photocatalysts is an efficient strategy for designing and fabricating novel photocatalysts with enhanced photo-response [17]. However, in most cases, hybrid photocatalysts exhibit visible-light absorption with a consequent reduction in band gaps [18,19]. Among various semiconducting photocatalysts, the two crystalline forms of zinc sulfide (ZnS) are some of the most important semiconductors. One crystalline form is cubic (Sphalerite), and the other is hexagonal (Wurtzite), with band gaps of 3.72 and 3.77 eV, respectively [20]. Zinc sulfide (ZnS) is an effective semiconductor material for photocatalytic degradation of pollutants due to its numerous advantages. ZnS exhibits high photocatalytic activity and can efficiently absorb light in the visible range, making it an effective catalyst for pollutant degradation. Additionally, ZnS is abundant and relatively inexpensive, making it a cost-effective option for large-scale applications. It is also chemically stable and corrosion-resistant, allowing it to withstand harsh environmental conditions. ZnS is non-toxic and environmentally friendly, making it a safer option compared to other toxic photocatalysts. Furthermore, ZnS can be synthesized in various forms, such as nanoparticles, nanorods, and thin films, making it versatile for use in different photocatalytic applications [21]. Recent research has shown that zinc oxide (ZnO) is capable of performing photocatalytic degradation of some organic pollutants. ZnO's unique properties include low cost, non-toxicity, and the ability to create photogenerated holes with high oxidation power to

destroy environmental pollutants. However, ZnO has a wide band gap (3.37 eV), which limits its performance in sunlight. When used as a catalyst, ZnO can only utilize about 3-5% of the UV light from solar energy for photocatalytic reactions [22]. Additionally, the fast recombination of photogenerated electron-hole pairs must be addressed for its application. Therefore, improving the photocatalytic performance of ZnO by reducing its band gap to enable absorption in the visible region and prevent the recombination of photogenerated electron-hole pairs has become an important research topic among universities and research institutes [23]. Several studies have investigated the photocatalytic activity of ZnS/ZnO heterostructures for the degradation of various dyes, such as Methylene blue, Rhodamine B, Congo Red, and Crystal Violet. For example, Fathi Sanad et al. synthesized ZnS/ZnO heterostructures using a sol-gel method. They demonstrated their enhanced photocatalytic activity for the degradation of Methylene Blue under visible light irradiation [24]. Li et al. fabricated porous ZnS, ZnO, and ZnS/ZnO nanosheets by thermal treatment of a ZnS precursor and applied them in Rhodamine B dye removal [25]. Sadollahkhani et al. studied the photocatalytic properties of ZnS/ZnO core-shell nanoparticles to degrade Congo Red dye at different pH values [26]. Additionally, Gupta et al. showed that ZnS/ZnO heterostructures have great potential for degrading dyes, as they applied a ZnS/ZnO heterosemiconductor in Crystal Violet dye removal [27]. Overall, ZnS/ZnO heterostructures have shown great potential for degrading dyes through their enhanced photocatalytic activity under both visible and UV light irradiation. The specific photocatalytic mechanism and efficiency depend on the specific heterostructure configuration and the type of dye being degraded. The ability to reuse a photocatalyst is crucial for practical applications of photocatalysis. Recovering and reusing the photocatalyst can reduce costs and waste, enhance performance, and improve the sustainability and economic viability of the process. This can be achieved through various methods such as immobilization, filtration, and surface modification or regeneration [24]. The objective of this study is to investigate the potential

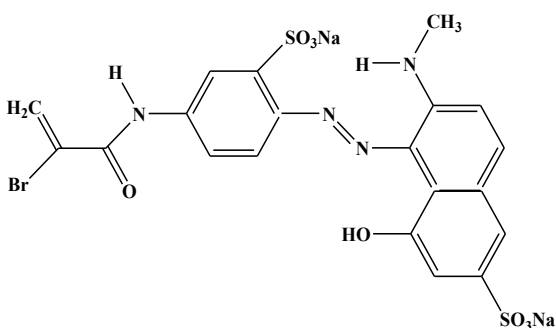
of photocatalytic removal of Reactive Red 66 dye using ZnS and ZnS/ZnO. It is necessary to mention that the application of ZnS and/or ZnS/ZnO photocatalysts in the degradation of Reactive Red 66 dye has not been explored before. Also, the ZnS/ZnO heterostructured semiconductor was prepared under mild conditions using a one-step reflux reaction between ZnCl<sub>2</sub> and Na<sub>2</sub>S in an ethyl pyridinium iodide ionic liquid media without the need for calcination [28]. The study examined the effect of various experimental parameters on dye removal, including pH, photocatalyst dosage, initial dye concentration, and contact time.

## 2. Materials and methods

### 2.1. Reagent and chemicals

All chemicals used in the experiments were of analytical grade and purchased from Merck Co. (Germany). The chemicals used in the study included zinc (II) chloride (ZnCl<sub>2</sub>), sodium sulfide hydrated (Na<sub>2</sub>S·9H<sub>2</sub>O), ethyl pyridinium iodide ionic liquid, hydrochloric acid (HCl), and ammonia (NH<sub>4</sub>OH). Reactive Red 66 was obtained from Nordex International, D.Z.E Dye Company (Austria), and used as received. Table 1 lists the properties of Reactive Red 66.

**Table 1.** Properties of Reactive Red 66.

Structure	
CAS registry number	12226-33-4
Physical state	Solid
Class	Single azo
Color	Red-purple
Empirical formula	C <sub>20</sub> H <sub>15</sub> BrN <sub>4</sub> Na <sub>2</sub> O <sub>8</sub> S <sub>2</sub>
Molecular weight	629.37 g/mol

### 2.2. Preparation of ZnS and ZnS/ZnO

The ZnS and ZnS/ZnO photocatalysts used in this study were produced according to the procedure reported in our previous work [28]. In brief, ZnS nanoparticles were prepared by reacting ZnCl<sub>2</sub> and Na<sub>2</sub>S·9H<sub>2</sub>O in a 1:2 molar ratio under reflux conditions for 1.5 hours. The ZnS/ZnO heterostructure was prepared by reacting ZnCl<sub>2</sub> and Na<sub>2</sub>S·9H<sub>2</sub>O in the presence of ethyl pyridinium iodide with a 1:4:4 molar ratio under reflux conditions for 4 hours.

### 2.3. Dye removal studies

The removal of Reactive Red 66 dye using ZnS and ZnS/ZnO heterostructures was analyzed using UV-Vis spectroscopy. The percentage of dye removal was investigated under both UV and visible light. In brief, 20 mL of a 20 mg/L solution of Reactive Red

66 in water was added to a beaker. Next, 0.02 g of ZnS and/or ZnS/ZnO photocatalysts were added. The pH of the solution was adjusted to 2, and the solution was irradiated under UV light for 30 minutes. The solution was then centrifuged, and the filtrate was monitored with a UV-Visible spectrophotometer at a wavelength of 514 nm. The effect of different parameters, including pH (2-8), photocatalyst dosage (0.02-0.03 g), dye concentration (5-60 ppm), and contact time (30-90 min), was investigated.

### 2.4. Recycle ability test

The dye removal efficiency was determined by measuring the dye concentration before and after adsorption. After the dye removal reaction, the photocatalyst was collected and washed with distilled water. The recovered photocatalyst was then dried in an oven at 60 °C for 1 h and reused

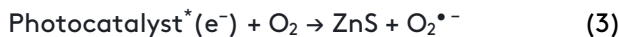
under optimal conditions for dye removal. The effect of three cycles was investigated for the photodegradation of Reactive Red 66.

### 3. Results and discussion

In our previous work [28], ZnS and ZnS/ZnO were characterized using various techniques, including Fourier transform infrared spectroscopy (FT-IR), X-ray diffraction (XRD), diffuse reflectance spectroscopy (DRS), field emission scanning electron microscope (FE-SEM), and energy-dispersive X-ray spectroscopy (EDS) mapping. The application of the prepared compounds in photocatalytic degradation was mentioned in the current study.

#### 3.1. Photodegradation using ZnS, and ZnS/ZnO structures

The photocatalytic degradation process of Reactive Red 66 using ZnS and/or ZnS/ZnO typically involves the following chemical reactions. Under UV radiation, the photo-induced electron-hole pairs were generated on the valance and conductive bands and transferred to the photocatalyst surface (1). The holes reacted with water molecules and formed hydroxyl radicals ( $\text{HO}^*$ ) (2). Photogenerated electrons from the photocatalyst generated the reduction reaction of  $\text{O}_2$  molecules to anionic superoxide radicals ( $\text{O}_2^{\bullet -}$ ) (3). Both radicals were highly reactive and effectively degraded the dye molecules and transformed them into  $\text{CO}_2$ ,  $\text{H}_2\text{O}$ , and degraded products.



The removal of Reactive Red 66 dye in the presence of ZnS and ZnS/ZnO composite was investigated through batch experiments using UV-Vis spectroscopy. A calibration curve was prepared based on the characteristic absorbance of the dye. The dye removal percentage was calculated from the following equation:

$$R = \frac{(C_0 - C_t)}{C_0} \times 100 \quad (4)$$

where  $C_0$  is the initial dye concentration (mg/L) and  $C_t$  is the dye concentration (mg/L) at time  $t$ .

##### 3.1.1. Effect of pH

It is well known that the pH of a solution affects both the form of compounds in water (aqueous chemistry) and the surface binding sites of adsorbents [29]. The effect of initial pH on the degradation of Reactive Red 66 was studied over a pH range of 2 to 8, with a constant initial dye concentration of 20 mg/L, an adsorbent dose of 0.02 g, and a UV irradiation time of 30 minutes. As shown in Fig. 1a and b, high pH values (alkaline media) decreased the photodegradation percentage of Reactive Red 66. The maximum uptake values were 70.7 and 91.7% using ZnS and ZnS/ZnO, respectively, indicating that dye removal was strongly dependent on pH. Alkaim et al. [30] reported that more  $\text{H}^+$  was available in acidic media, improving the electrostatic attraction.

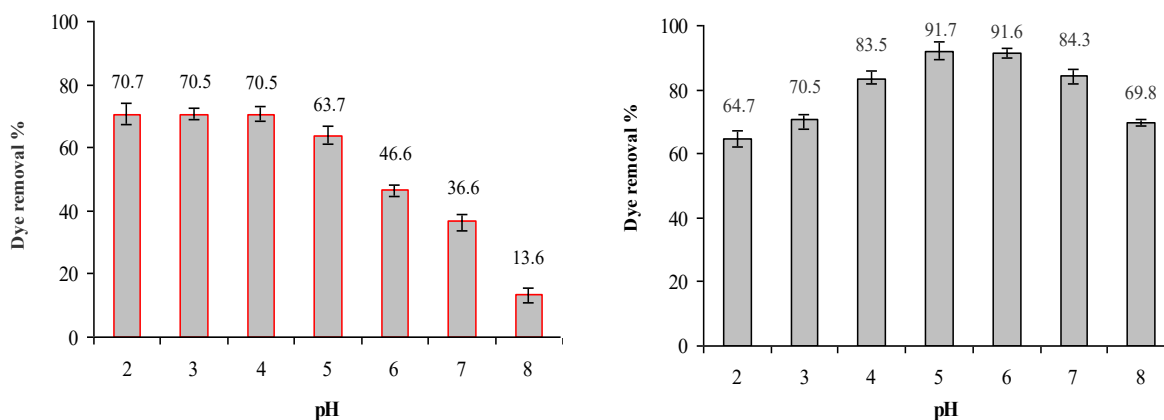


Fig. 1. Effect of pH on the degradation of Reactive Red 66 using ZnS (a) and ZnS/ZnO (b).

### 3.1.2. Effect of photocatalyst dosage

The effect of ZnS and ZnS/ZnO dosage (0.02-0.03 g) on the photodegradation of Reactive Red 66 at a concentration of 20 mg/L of dye was studied. The results showed that as the photocatalyst dosage increased, the degradation percentage increased from 70.1 to 77.7% and from 74.2 to 90.7% using ZnS and ZnS/ZnO, respectively (Figure 2a, b). However, it was observed that as the dosage of ZnO and ZnS/ZnO increased to 0.032 g and 0.028 g, respectively, there was a decrease in the dye removal percentage from 77.7 to 75.9% and from 90.7 to 82.0%. These results indicate that an excess of the photocatalyst causes active site saturation.

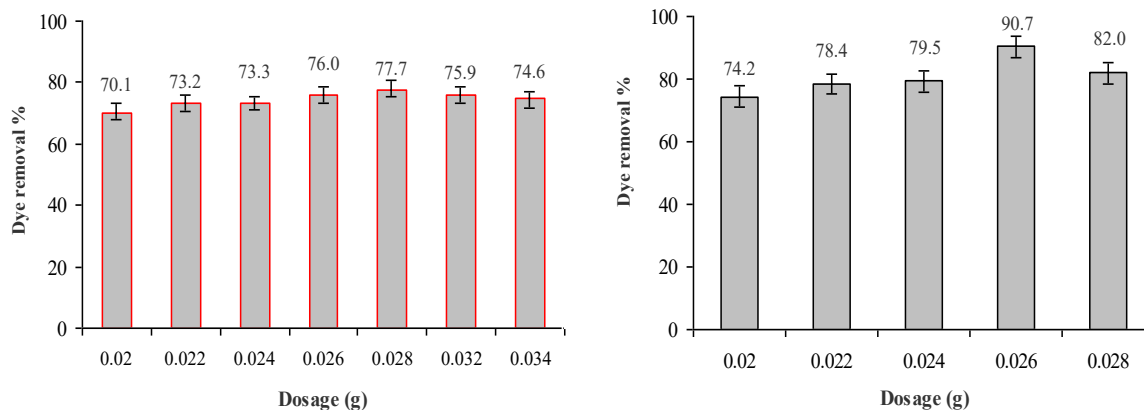


Fig. 2. Effect of photocatalyst dosage on the degradation of Reactive Red 66 using ZnS (a) and ZnS/ZnO (b).

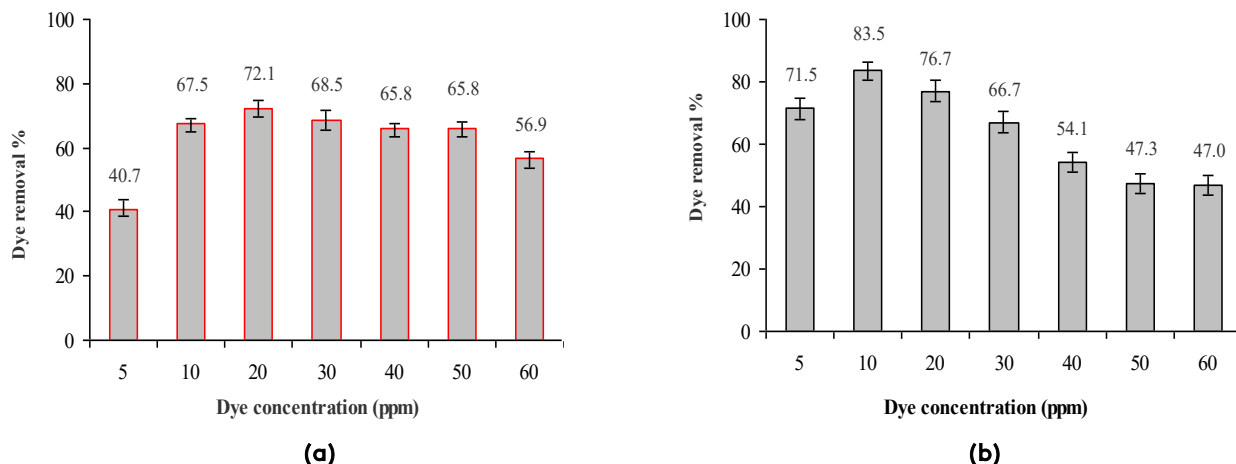


Fig. 3. Effect of dye concentration on the degradation of Reactive Red 66 using ZnS (a) and ZnS/ZnO (b).

### 3.1.4. Effect of contact time

In the next step, the effect of contact time on dye removal was investigated under optimal conditions (pH of 2 and 5, photocatalyst dosage of 0.028 and 0.026 g, initial dye concentration of 10 and 20 mg/L for ZnS and ZnS/ZnO, respectively). The removal percentage versus contact time was studied in the

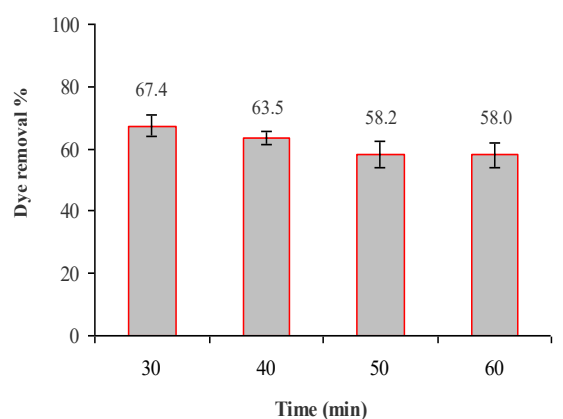
### 3.1.3. Effect of initial dye concentration

The effect of the initial dye concentration (5-60 mg/L) on Reactive Red 66 removal was examined (Figures 3a, b). The results show that photodegradation increased at lower dye concentrations. The maximum percentage of photodegradation was 72.1% and 83.5% using ZnS and ZnS/ZnO photocatalysts, respectively. The degradation rate of Reactive Red 66 changed as the initial dye concentration increased from 5-60 mg/L, with values of 40.7, 67.5, 72.1, 68.5, 65.8, 65.4, and 56.9% using the ZnS photocatalyst. The dye removal percentages were 71.5, 83.5, 76.7, 66.7, 54.1, 47.3, and 47% using ZnS/ZnO.

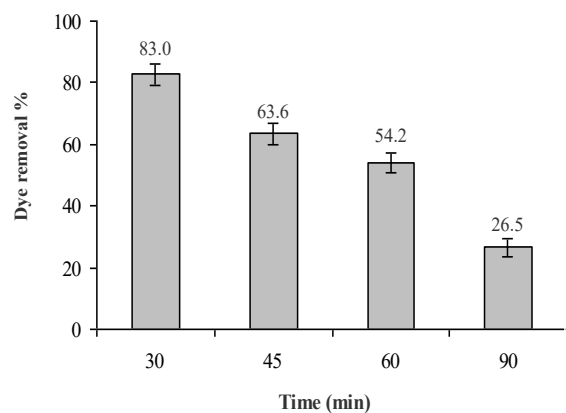
range of 30-90 min (Figures 4a, b). The dye removal percentage of Reactive Red 66 by ZnS significantly increased up to 30 min, and then the dye removal slowed until equilibrium was reached. After 30 min, the maximum dye removal of Reactive Red 66 was obtained for ZnS (67.4%) and ZnS/ZnO (83%). At the beginning of the process, the absorption rate

was high due to the surface absorption of dye molecules, which gradually decreased with the occupation of the surface functional groups and vacant pores. The many empty pores of the photocatalysts were mainly responsible for the adsorption, followed by photodegradation. Therefore, 30 min was chosen as the optimal contact time in this study.

The dye removal efficiency was determined using ZnS and ZnS/ZnO under visible light (Figure 5). The results showed that the presence of the ZnS/ZnO heterostructure semiconductor favored the photodegradation process under visible light, with a removal efficiency of 75.22% after one week.



(a)



(b)

**Fig. 4.** Effect of contact time on the degradation of Reactive Red 66 using ZnS (a) and ZnS/ZnO (b).

### 3.2. Recyclability of adsorbent

Regeneration and recyclability of the photocatalyst play an important role from an economic and practical point of view. In this study, the ZnS and ZnS/ZnO photocatalysts were reused for dye removal in three cycles. The results of the

adsorbent's reusability are illustrated in Figure 6. It is noteworthy that the removal percentage after three cycles was above 12.2 and 37.7% for ZnS and ZnS/ZnO, respectively.

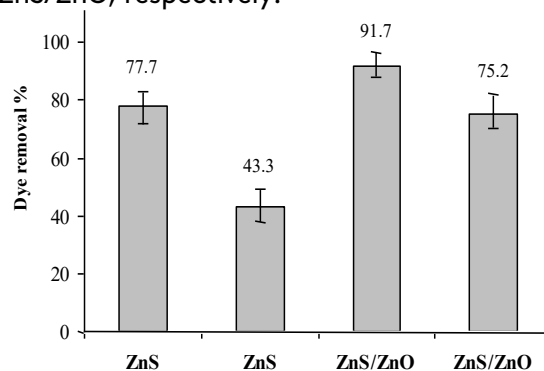
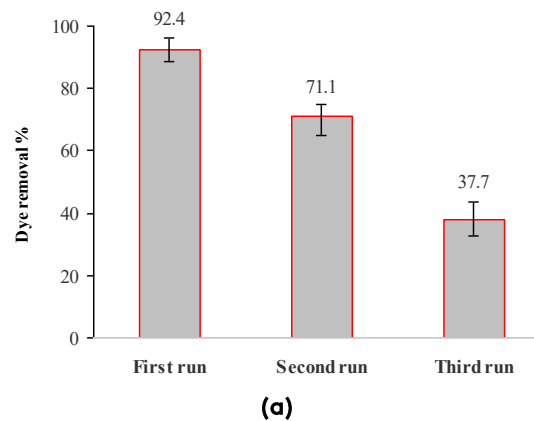
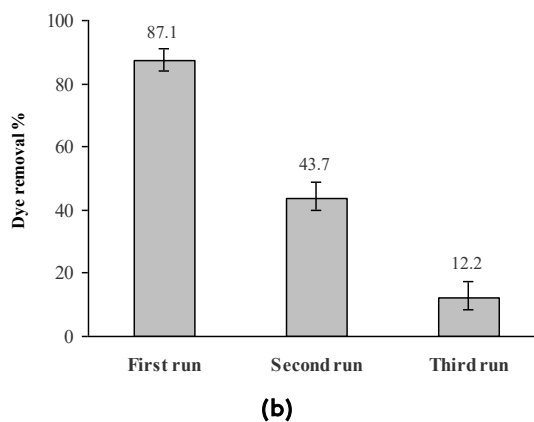


**Fig. 5.** Reactive Red 66 removal using ZnS and ZnS/ZnO under UV and visible light.



(a)



(b)

**Fig. 6.** Recyclability study of photocatalyst for the Reactive Red 66 removal using ZnS (a) and ZnS/ZnO (b).

## 4. Conclusions

Photodegradation is the most efficient process for dye removal. In this study, ZnS and a ZnS/ZnO heterosemiconductor were investigated for Reactive Red 66 removal from aqueous media. Several factors, including the pH level of the

solution, the dosage of the used photocatalyst, the concentration of dye present, and the duration of contact time, influenced the extent of dye removal. The results revealed that the low pH values of the solution increased the dye removal percentage of Reactive Red 66. Furthermore, it was observed that the percentage of dye degradation increased with an increase in the dosage of the photocatalyst. However, the percentage of dye removal showed a decreasing trend as the dosage of ZnO and ZnS/ZnO was increased to 0.032 and 0.028 g, respectively. The degradation rate of Reactive Red 66 was found to decrease as the initial dye concentration was increased to 20 and 30 ppm when using ZnS and ZnS/ZnO, respectively. The findings indicated that the ZnS/ZnO photocatalyst was more effective in removing Reactive Red 66 through the photodegradation process compared to ZnS alone, exhibiting a high removal efficiency of 91.7%. The amount of dye removed under visible light was measured to be 75.2%. The results demonstrate that the ZnS/ZnO heterostructure has promising potential as a dye absorbent. In the future, this composite can be further examined and evaluated for the removal of other dye pollutants.

### Acknowledgement

The authors would like to acknowledge the financial support from the Yadegar-e-Imam Khomeini (RAH) Shahre Rey Branch, Islamic Azad University.

### References

- [1] Dinari, A., Mahmoudi, J. (2022). Response surface methodology analysis of the photodegradation of methyl orange dye using synthesized TiO<sub>2</sub>/Bentonite/ZnO composites. *Advances in Environmental Technology*, 1, 31-46.  
<https://doi.org/10.22104/AET.2022.5204.1409>
- [2] Ilbeigi Asl, M., Mehdipour Ghazi, M., Jahangiri, M. (2016). Synthesis, characterization and degradation activity of Methyl orange Azo dye using synthesized CuO/ $\alpha$ -Fe<sub>2</sub>O<sub>3</sub> nanocomposite. *Advances in Environmental Technology*, 3, 143-151.  
<https://doi.org/10.22104/AET.2017.427>
- [3] Pavel, M., Anastasescu, C., State, R.N., Vasile, A., Papa, F., Balint, I. (2023). Photocatalytic degradation of organic and inorganic pollutants to harmless end products: assessment of practical application potential for water and air cleaning. *Catalysts*, 13(2), 380.  
<https://doi.org/10.3390/catal13020380>
- [4] Ramalingam, G., Perumal, N., Priya, A.K., Rajendran, S. (2022). A review of graphene-based semiconductors for photocatalytic degradation of pollutants in wastewater. *Chemosphere*, 300, 134391.  
<https://doi.org/10.1016/j.chemosphere.2022.134391>
- [5] Kang, W., Chen, S., Yu, H., Xu, T., Wu, S., Wang, X., Lu, N., Quan, X., Liang, H. (2021). Photocatalytic ozonation of organic pollutants in wastewater using a flowing through reactor. *Journal of Hazardous Materials*, 405, 124277.  
<https://doi.org/10.1016/j.jhazmat.2020.124277>
- [6] Preda, S., Umek, P., Zaharescu, M., Anastasescu, C., Petrescu, S.V., Gifu, C., Eftimie, D.-I., State, R., Papa, F., Balint, I. (2022). Iron modified titanate nanorods for oxidation of aqueous ammonia using combined treatment with ozone and solar light irradiation. *Catalysts*, 12, 666.  
<https://doi.org/10.3390/catal12060666>
- [7] Mirsadeghi, S., Zandavar, H., Rajabi, H.R., Sajadiasl, F., Ganjali, M.R., Pourmortazavi, S.M. (2021). Superior degradation of organic pollutants and H<sub>2</sub>O<sub>2</sub> generation ability on environmentally-sound constructed Fe<sub>3</sub>O<sub>4</sub>-Cu nanocomposite. *Journal of Materials Research and Technology*, 14, 808-821.  
<https://doi.org/10.1016/j.jmrt.2021.07.007>
- [8] Qu, Y., Chen, Z., Duan, Y., Liu, L. (2022). H<sub>2</sub>O<sub>2</sub> assisted photocatalysis over Fe-MOF modified BiOBr for degradation of RhB. *Journal of Chemical Technology and Biotechnology*, 97, 2881-2888.  
<https://doi.org/10.1002/jctb.7199>
- [9] Wang, X., Li, S., Chen, P., Li, F., Hu, X., Hua, T. (2022). Photocatalytic and antifouling properties of TiO<sub>2</sub>-based photocatalytic membranes. *Materials Today Chemistry*, 23, 100650.  
<https://doi.org/10.1016/j.mtchem.2021.100650>
- [10] Chemin, J.-B., Bulou, S., Baba, K., Fontaine, C., Sindzingre, T., Boscher, N.D., Choquet, P. (2018). Transparent anti-fogging and self-

- cleaning TiO<sub>2</sub>/SiO<sub>2</sub> thin films on polymer substrates using atmospheric plasma. *Scientific Reports*, 8, 9603.  
<https://doi.org/10.1038/s41598-018-27526-7>
- [11] He, F., Jeon, W., Choi, W. (2021). Photocatalytic air purification mimicking the self-cleaning process of the atmosphere. *Nature Communications*, 12, 2528.  
<https://doi.org/10.1038/s41467-021-22839-0>
- [12] Sharma, S., Kumar, R., Raizada, P., Ahamad, T., Alshehri, S.M., Nguyen, V.-H., Thakur, S., Nguyen, C.C., Kim, S.Y., Le, Q.V., Singh, P. (2022). An overview on recent progress in photocatalytic air purification: metal-based and metal-free photocatalysis. *Environmental Research*, 214, 113995.  
<https://doi.org/10.1016/j.envres.2022.113995>
- [13] Ren, G., Han, H., Wang, Y., Liu, S., Zhao, J., Meng, X., Li, Z. (2021). Recent advances of photocatalytic application in water treatment: a review. *Nanomaterials*, 11(7), 1804.  
<https://doi.org/10.3390/nano11071804>
- [14] Li, X., Yu, J. Jaroniec, M. (2016). Hierarchical photocatalysts. *Chemical Society Reviews*, 45, 2603-2636.  
<https://doi.org/10.1039/C5CS00838G>
- [15] Zhang, X., Wang, Y., Liu, B., Sang, Y., Liu, H. (2017). Heterostructures construction on TiO<sub>2</sub> nanobelts: a powerful tool for building high-performance photocatalysts. *Applied Catalysis B: Environmental*, 202, 620-641.  
<https://doi.org/10.1016/j.apcatb.2016.09.068>
- [16] Lin, Y.-F., Hsu, Y.-J. (2013). Interfacial charge carrier dynamics of type-II semiconductor nanoheterostructures. *Applied Catalysis B: Environmental*, 130, 93-98.  
<https://doi.org/10.1016/j.apcatb.2012.10.024>
- [17] Yousaf, A.B., Imran, M., Zaidi, S.J., Kasak, P., Ansari, T.M., Manzoor, S., Yasmeen, G., (2017). Synergistic effect of interfacial phenomenon on enhancing catalytic performance of Pd loaded MnO<sub>x</sub>-CeO<sub>2</sub>-C hetero-nanostructure for hydrogenation and electrochemical reactions. *Journal of Materials Chemistry A*, 5, 10704-10712.  
<https://doi.org/10.1039/C7TA02122D>
- [18] Yousaf, A.B., Imran, M., Zaidi, S.J., Kasak, P. (2017). Highly efficient photocatalytic Z-scheme hydrogen production over oxygen-deficient WO<sub>3-x</sub> nanorods supported Zn<sub>0.3</sub>Cd<sub>0.7</sub>S heterostructure. *Scientific Reports*, 7, 6574.  
<https://doi.org/10.1038/s41598-017-06808-6>
- [19] Imran, M., Yousaf, A.B., Kasak, P., Zeb, A., Zaidi, S.J. (2017). Highly efficient sustainable photocatalytic Z-scheme hydrogen production from an  $\alpha$ -Fe<sub>2</sub>O<sub>3</sub> engineered ZnCdS heterostructure. *Journal of Catalysis*, 353, 81-88.  
<https://doi.org/dx.doi.org/10.1016/j.jcat.2017.06.019>
- [20] Lee, G.-J., Wu, J.J. (2017). Recent developments in ZnS photocatalysts from synthesis to photocatalytic applications - A review. *Powder Technology*, 318, 8-22.  
<https://doi.org/10.1016/j.powtec.2017.05.022>
- [21] Isac, L., Enesca, A. (2022). Recent developments in ZnS-based nanostructures photocatalysts for wastewater treatment. *International Journal of Molecular Sciences*, 23(24), 15668.  
<https://doi.org/10.3390/ijms232415668>
- [22] Ma, H., Cheng, X., Ma, C., Dong, X., Zhang, X., Xue, M., Zhang, X., Fu, Y. (2013). Synthesis, characterization, and photocatalytic activity of N-doped ZnO/ZnS composites. *International Journal of Photoenergy*, 625024.  
<https://doi.org/10.1155/2013/625024>
- [23] Jiang, X., Huang, L., Li, L., Zhang, L., Guo, X., Li, Y., Sun, X. (2021). A novel strategy to construct the superior performance of 3D multi-shell CeO<sub>2</sub>/ZnO@ZnS as a reusable sunlight-driven ternary photocatalyst for highly efficient water remediation. *Journal of Environmental Chemical Engineering*, *Journal of Environmental Chemical Engineering*, 9, 105608.  
<https://doi.org/10.1016/j.jece.2021.105608>
- [24] Fathi Sanad, M., Shalan, A.E., Magdy Bazid, S., Abdelbasir, S.M. (2018). Pollutant degradation of different organic dyes using the photocatalytic activity of ZnO@ZnS nanocomposite materials. *Journal of Environmental Chemical Engineering*, 6 (4), 3981-3990.  
<https://doi.org/10.1016/j.jece.2018.05.035>
- [25] Li, X., Li, X., Zhu, B., Wang, J., Lan, H., Chen, X. (2017). Synthesis of porous ZnS, ZnO and ZnS/ZnO nanosheets and their photocatalytic

- properties, *RSC Advances*, **7**, 30956-30962. <https://doi.org/10.1039/C7RA03243A>
- [26] Sadollahkhani, A., Nur, O., Willander, M., Kazeminezhad, I., Khranovskyy, V., Eriksson, M.O., Yakimova, R., Holtz P.-O. (2015). A detailed optical investigation of ZnO@ZnS core-shell nanoparticles and their photocatalytic activity at different pH values. *Ceramics International*, **41**(5), 7174-7184. <https://doi.org/10.1016/j.ceramint.2015.02.040>
- [27] Gupta, A., Kaur, J., Prakash Pandey, O. (2023). A comparative study of ZnS-ZnO nanocomposite assembly for photocatalytic removal of crystal violet dye. *Phys. Status Solidi A*, **220**, 2300028. <https://doi.org/10.1002/pssa.202300028>
- [28] Sheshmani, S., Mardali, M., Shahvelayati, A.S., Hajiaghababaei, L. (2022). ZnS/ZnO heterostructure semiconductor: Promising approach through ionic liquid media without calcination. *Journal of Particle Science and Technology*, **8**, 115-119. <https://doi.org/10.22104/JPST.2023.6214.1226>
- [29] Ashori, A., Hamzeh, Y., Ziapour, A. (2014). Application of soybean stalk for the removal of hazardous dyes from aqueous solutions. *Polymer Engineering and Science*, **54** (1), 239-245. <https://doi.org/10.1002/pen.23695>
- [30] Alkaim, A.F., Aljebori, A.M., Alrazaq, N.A., Baqir, S.J., Hussein, F.H., Lilo, A.J. (2014). Effect of pH on adsorption and photocatalytic degradation efficiency of different catalysts on removal of methylene blue. *Asian Journal of Chemistry*, **26**, 8445-8448. <http://dx.doi.org/10.14233/ajchem.2014.17908>